Journal of Statistical Physics, Vol. 124, No. 1, July 2006 (© 2006)
DOI: 10.1007/s10955-006-9149-0

Anderson Localization, Non-linearity and Stable Genetic Diversity*

Charles L. Epstein[1]

Received March 29, 2006; accepted June 1, 2006
Published Online: July 12, 2006

In many models of genotypic evolution, the vector of genotype populations satisfies a system of linear ordinary differential equations. This system of equations models a competition between differential replication rates (fitness) and mutation. Mutation operates as a generalized diffusion process on genotype space. In the large time asymptotics, the replication term tends to produce a *single* dominant quasi-species, unless the mutation rate is too high, in which case the asymptotic population becomes de-localized. We introduce a more macroscopic picture of genotypic evolution wherein a random fitness term in the linear model produces features analogous to Anderson localization. When coupled with density dependent non-linearities, which limit the population of any given genotype, we obtain a model whose large time asymptotics display stable genotypic diversity.

KEY WORDS: quasi-species, spin glass models, non-linearity, Anderson localization, genotypic diversity, paramuse model, Eigen model

1. INTRODUCTION

Explaining the persistence of biological diversity is a longstanding problem of considerable interest in evolutionary theory, see e.g. see Refs. 6 and 18. This paper contains a proposal for a class of theories of genotypic evolution that display stable, arbitrarily complex, genetic diversity. Our models are built out of pieces that have been on the shelves for quite a while, but perhaps have not before been placed together.

*Research partially supported by DARPA under the FUNBIO program and the Francis J. Carey Term Chair.

[1] Department of Mathematics and Laboratory for Structural NMR Imaging, University of Pennsylvania, Pennsylvania

We start out with linear "spin glass" models, which cast genotypic evolution as competing processes of replication and mutation, see Refs. 3, 4, 12, 20, 23. Suppose that the possible genotypes are labeled by the integers $\{1, \ldots, N\}$ and $\mathbf{P}(t) = (P_1(t), \ldots, P_N(t))$ is a vector, with $P_j(t)$ the population of genotype j at time t. The standard linear model for genotypic evolution is a system of ordinary differential equations:

$$\frac{d\mathbf{P}(t)}{dt} = (R + M)\mathbf{P}(t). \tag{1}$$

Here M describes the process of mutation and R the net replication rate of each genotype; it is called the "fitness matrix." For reasonable evolutionary models, the largest eigenvalue, λ_{PF}, of the combined system $R + M$, (called the Perron-Frobenius eigenvalue) corresponds to a positive eigenvector $\mathbf{v}_{\mathrm{PF}}$. An eigenvector that is highly localized near a single genotype is said to represent a quasi-species. In the large time limit, the solution to (1) behaves like $\langle \mathbf{P}(0), \mathbf{v}_{\mathrm{PF}} \rangle e^{\lambda_{\mathrm{PF}} t}$. Hence, either the population is de-localized, or the fastest replicating quasi-species dominates. In either case there is no plurality of well defined quasi-species.

We posit the existence of fitness matrices so that, if $\|M\|$ is sufficiently small, then the combined replication-mutation system exhibits properties, in the limit of large genome length, analogous to Anderson localization, see Refs. 2, 5, 17, 22. This means that, if $\{\lambda_1 \leq \lambda_2 \leq \ldots < \lambda_N\}$ are the eigenvalues of $R + M$ and $\{\psi_\alpha\}$ the corresponding eigenvectors, then, for eigenvalues close to $\lambda_N = \lambda_{\mathrm{PF}}$, the eigenvectors are highly localized and their overlaps are not correlated with the differences $\{|\lambda_\alpha - \lambda_\beta|\}$. Such a model already exhibits a weak form of genetic diversity, having a large number of well defined, well separated, "long-lived" quasi-species.

As noted, in a linear model it is inevitable that in the long run, either a single quasi-species comes to dominate, or localization breaks down and there are no well defined quasi-species. To address this, we add a density dependent quadratic term and a constant F, that limit the growth of any given genotype, and select out a certain subset of long lived quasi-species. The model we obtain is the non-linear ODE system:

$$\frac{d\mathbf{P}}{dt}(t) = (R + M + F)\mathbf{P}(t) - b\mathbf{P}. * \mathbf{P}(t), \tag{2}$$

where $[\mathbf{P}. * \mathbf{P}]_j = P_j^2$. We call F the environmental *fecundity*, as it is a measure of the potential for quasi-species diversity. This step is suggested by a paper of Nelson and Shnerb, where they show, in a continuum population biology model, that such a term, when coupled to Anderson localization does in fact lead to an asymptotic state with stable diversity, see Ref. 15.

In this paper we consider questions related to the long time macroscopic structure of genotypic evolution. Our results can be seen as providing a

mathematical correlate to, though not a precise model for, the digital evolution experiments described in Ref. 6, wherein resource limitations produce stable genetic diversity. We focus on aspects of linear models that are connected to the randomness of the fitness matrix, and beyond that, on the consequences of non-linear corrections that may be seen as accounting for the finiteness of resources.

The main contribution of this paper is to put these two pieces together in the context of genotypic evolution and suggest potentially fruitful directions for further research in both evolution and spectral theory. In small numerical examples we show that our localization hypothesis is not unreasonable, and that the non-linear model behaves as predicted. The rigorously established results showing that localization occurs for Schrödinger operators with sufficiently weak diffusion, and that, when it occurs, it is generic, give support for the idea that such models should exist and that the localization property should be insensitive to the details of the model. Finally, there is a certain sublime beauty to a world in which the *complexity* of the mapping from genotype to fitness conspires with environmental *limitations* on population size to produce stable genetic diversity.

2. LINEAR MODELS

Recently there has been a great deal of interest in the connections between various models that arise in statistical mechanics and models of genetic evolution. Early models were defined by Eigen and Crow-Kimura, see Refs. 3, 7, 8, 11. For a good survey of this subject with many further references to the literature see Ref. 13. Genotypes are described as finite sequences $(s_1, \ldots, s_n)$, where the entries $\{s_j\}$ are drawn from a finite alphabet. For example, if one wishes to model chromosomal evolution, then the alphabet is that of nucleotides $\{A, C, G, T\}$ (or, for RNA, $\{A, C, G, U\}$). If one wishes to study protein evolution, then one might use the list of the 20 amino acids. In the interest of simplicity, most investigators simply use a two letter alphabet, which can be thought of as purines and pyrimidines. We follow that convention, but our main results also apply to models using any finite length alphabet. Let $\mathcal{G}_n$ denote the set of possible genotypes of length n expressed in the given fixed alphabet with 2 members. If all genotypes are possible, then $|\mathcal{G}_n| = 2^n$. In the sequel we let $N = 2^n$. In this case a genotype can be represented as a string of 0s and 1s and so can interpreted as a binary representation of a positive integer. The genotypes can therefore be labeled by the set of integers $\mathcal{J}_n = \{1, 2, \ldots, N\}$, though this labeling scheme is entirely arbitrary and conveys no "invariant" information.

One way to specify a model for mutation from one genotype to another is by assigning probabilities $\{m_{ij} : i \neq j \in \mathcal{J}_n\}$ that, in a given unit of time, the genotype S_i mutates to the genotype S_j. As above, $P_j(t)$ is the population of genotype S_j at time t. In addition to mutation, each genotype has a replication

rate, r_j, so that, in the absence of mutation, $P_j(t)$ would satisfy:

$$\frac{dP_j}{dt} = r_j P_j(t). \tag{3}$$

Hence r_j is the difference of the birth and death rates for the genotype S_j; it summarizes the fitness of the genotype. The *fitness* matrix, R, is defined to be

$$R_{ij} = \begin{cases} 0 & \text{if } i \neq j \\ r_i & \text{if } i = j. \end{cases} \tag{4}$$

In parallel models, the mutational process is described by the *mutation* matrix, M, given by:

$$M_{ij} = \begin{cases} m_{ji} & \text{if } i \neq j \\ -\sum_{k \neq i} m_{ik} & \text{if } i = j. \end{cases} \tag{5}$$

The negative diagonal term is required so that the total mutational flux out of a given genotype, is balanced by an equal decrease in its population. A linear, parallel model for the time course of the genotype *populations* is then

$$\frac{d\mathbf{P}}{dt} = R\mathbf{P} + M\mathbf{P}. \tag{6}$$

In many prior papers, this model is described by a non-linear ordinary differential equation for the population *densities*,

$$\mathbf{p}(t) = \frac{\mathbf{P}(t)}{\sum_{j=1}^{N} P_j(t)}, \tag{7}$$

rather than the populations themselves. These non-linear models are equivalent, under a simple change of variables, to linear models, and it is the linear models that are amenable to analysis.[2]

If $S_i = (s_1, \ldots, s_n)$, $S_j = (s'_1, \ldots, s'_n)$ are two genotypes, then the Hamming distance between them, $d_H(S_i, S_j)$, equals the number of entries where they differ. The mutation probabilities are often taken to be functions of the Hamming distance. In the paramuse model the mutation matrix is specified by

$$M_{ij} = \begin{cases} \mu & \text{if } d_H(S_i, S_j) = 1 \\ -n\mu & \text{if } i = j \\ 0 & \text{otherwise.} \end{cases} \tag{8}$$

[2] The model for population densities determined by (6) is

$$\frac{d\mathbf{p}(t)}{dt} = (R + M)\mathbf{p}(t) - \langle R\mathbf{p}(t), \mathbf{1}\rangle \mathbf{p}(t), \tag{9}$$

where $\mathbf{1} = (1, \ldots, 1)$. The non-linear term serves only to keep the sum $\langle \mathbf{p}(t), \mathbf{1}\rangle = \sum_j p_j(t)$ equal to 1.

The probability-per-unit-time of changing one letter is μ and the probability-per-unit-time of changing more than one letter is zero.

A second class of models derives from the Eigen model. In this case, the mutation rate is a function of the Hamming distance of the form

$$Q_{ij} = q^n \left(\frac{1-q}{q}\right)^{d_H(S_i,S_j)} . \tag{10}$$

The assumption here is that probability-per-unit-time of a mutation occurring at each site on the genome is equal to $1-q$, and that the different sites mutate independently of one another. In the Eigen model, the population satisfies the differential equation

$$\frac{d\mathbf{P}}{dt} = (QR - D)\mathbf{P}, \tag{11}$$

here D is a second diagonal matrix, which describes the rate of degradation of a given genotype. In this model, the mutation process *follows* the replication process, rather than the two occurring in parallel. If $q \sim n/(n+\mu)$, then the qualitative behavior of solutions to (11) is quite similar to the solutions of the paramuse model.[3]

In our subsequent analysis we stick to the representation given in (6). The precise nature of M is less important than the assumption that the matrices $\{e^{tM} : t > 0\}$ should have the qualitative properties of a diffusion process in that they should be positivity improving, i.e. if $\mathbf{P}_0$ is a vector with non-negative coefficients, then $e^{tM}\mathbf{P}_0$ has positive coefficients. For finite matrices, this condition essentially amounts to the requirement that the off-diagonal entries of M are non-negative. One also expects the matrix elements M_{ij} to decrease rapidly as $d_H(S_i, S_j)$ grows.

In these models, a quasi-species is represented by a population vector, $\mathbf{P}$, that is highly concentrated around a single vertex or small cluster of nearby vertices, in the sense of Hamming distance, see Refs. 9, 10, 14. A population vector with several such clusters, which are well separated, would then represent a collection of quasi-species. As remarked above, the mutation process is like a diffusion. The eigenvectors of the matrix M are not localized, and the Perron-Frobenius Theorem implies that the largest eigenvalue of M, ν_{PF}, corresponds to an eigenvector $\mathbf{u}_{\mathrm{PF}}$ all of whose entries are positive; usually $\sqrt{N}\mathbf{u}_{\mathrm{PF}} = (1, \ldots, 1)$. Under the effects of

[3] A priori, this model looks rather different from (6) with M defined in 8, but if we make the substitution $\mathbf{W} = \sqrt{R}\mathbf{P}$, then

$$\frac{d\mathbf{W}}{dt} = (\sqrt{R}Q\sqrt{R} - D)\mathbf{W}, \tag{12}$$

so that the matrix on the right hand side is again symmetric, with non-negative, rapidly decaying off-diagonal entries. With $q \sim n/(n+\mu)$, the matrix $\sqrt{R}Q\sqrt{R} - D = (R-D) + O(\mu)$, so, for small μ, the general character of the model is again determined by the distribution of entries along the diagonal of $R - D$.

mutation *alone*, any initially non-negative population, $\mathbf{P}_0$, behaves asymptotically as

$$\mathbf{P}(t) \sim \langle \mathbf{P}_0, \mathbf{u}_{\mathrm{PF}} \rangle \mathbf{u}_{\mathrm{PF}} e^{\nu_{\mathrm{PF}} t}. \tag{13}$$

So the effect of the mutational process is to smear out the population and destroy any localized populations that might be present in the initial distribution of genotypes.

On the other hand, the fitness matrix R is diagonal; if it has distinct entries, then each basis vector $e_j = (0, \ldots, 0, 1, 0, \ldots, 0)$ (a single 1 in the jth place) defines a quasi-species. In the absence of mutation, the population of this quasi-species evolves as $e^{r_j t} P_j(0)$. The matrix $(R + M)$ is also positivity improving, and hence has a positive Perron-Frobenius eigenvector, $\mathbf{v}_{\mathrm{PF}}$, corresponding to the largest eigenvalue, λ_{PF}. If $\mathbf{v}_{\mathrm{PF}}$ is localized, then this is a quasi-species with replication rate λ_{PF}. From our perspective, the problem here is that, in the long time limit, the population will again satisfy $\mathbf{P}(t) \sim \langle \mathbf{P}_0, \mathbf{v}_{\mathrm{PF}} \rangle \mathbf{v}_{\mathrm{PF}} e^{\lambda_{\mathrm{PF}} t}$, and be dominated by the population distribution (quasi-species or not) with this highest replication rate.

In most prior analyses of these models, this was not viewed as a difficulty, for the problem under analysis was the stability of a single quasi-species under various levels of mutation, with different choices of simple fitness landscapes, having a small number of minima and maxima. This sort of analysis can be regarded as focusing on a small neighborhood of a vertex in $\mathcal{G}_n$: If we assume that $m << n$ sites participate in the evolutionary process, then the analysis proceeds on $\mathcal{G}_m$ viewed as a subgraph of $\mathcal{G}_n$. On this subgraph (length scale), even a macroscopically random fitness landscape could well appear quite simple. Hence, thermodynamic analyses, like those in Refs. 16 and 20, can be viewed as genotypically localized, short time analyses that take place within the larger macroscopic framework of genetic evolution.

3. ANDERSON LOCALIZATION

The combined linear model given in (6) represents a competition between the replication term, which, if the diagonal entries are distinct, tends to preserve quasi-species, and the mutation term, which tends to destroy them. As such, these models have a great deal in common with the models for conduction in semiconductors studied by Anderson. He considered models similar to

$$\partial_t u(x, t) = (\mu \Delta + q(x) + E) u(x, t), \tag{14}$$

where $u(x, t)$ is a non-negative function defined on $\mathbb{R}^d$, Δ is the standard Laplace operator, and $q(x)$ is a bounded "random" potential. This does not mean that $q(x)$ is an irregular function, but rather that it is non-periodic and lacking any simple asymptotic behavior as $\|x\|$ tends to infinity. (A simple example in 1D is

$\cos x + \cos \sqrt{2}x$.) From Anderson's seminal work and many subsequent analyses, it has become clear that there is a very fundamental and generic localization property shared by systems with $q(x)$ a random "potential." It is an analogue of this property that we posit for our linear models.

For each genome length n, we suppose that the fitness matrix R_n is random, constantly varying throughout genotype space and neither periodic nor with any asymptotic behavior. This does not preclude the fitness landscape from being locally smooth or having large regions where it is approximately constant. We let $\{L_n = R_n + M_n : n = 1, 2, \ldots\}$ denote a sequence of linear operators acting on functions on $\mathcal{G}_n$. In our subsequent analysis we use the following

localization ansatz:

> As n tends to infinity, the spectrum of the operators L_n becomes dense in some interval with right end point $\lambda_N = \sup \mathrm{spec}(L_n)$. The corresponding normalized eigenvectors become exponentially localized, with the overlaps in support uncorrelated to differences in the eigenvalues.

Operationally, the localization ansatz is that, for large enough n, L_n has a large number of eigenvalues close to λ_N, such that the corresponding normalized eigenvectors $\{\psi_\alpha\}$ are highly localized, and the overlaps in their supports are uncorrelated with the differences $\{|\lambda_\alpha - \lambda_\beta|\}$. Quantitatively we take this to mean that for each α, there is a $j_\alpha \in \mathcal{J}_n$ and positive numbers ξ_α, C_α, so that

$$|\psi_\alpha(j)| < C_\alpha e^{-\frac{d_H(j, j_\alpha)}{\xi_\alpha}}, \tag{15}$$

and $d_H(j_\alpha, j_\beta)$ is large, with high probability, if $|\lambda_\alpha - \lambda_\beta|$ is small. Moreover, we assume that the numbers $\{\psi_\alpha(j) : j \in \mathcal{J}_n\}$ are positive for most values of j. Because of exponential localization, this assumption does not contradict the fact that the eigenvectors are an orthonormal set.

One might want to suppose that the matrices $\{R_n\}$ converge to an infinite diagonal matrix R_∞, and the sequence of mutation matrices $\{M_n\}$ converge, in some sense, to an operator M_∞ acting on ℓ^2, so that one could speak of the behavior of the limiting operator $L_\infty = R_\infty + M_\infty$. As each genotype in $\mathcal{G}_\infty$ has infinitely many nearest neighbors, it is by no means obvious how to normalize the sequence $\{M_n\}$ so that the limit produces a non-trivial diffusion process. At realistic mutation rates, genotype space seems to be explored very slowly, so there is not much practical difference between a very large, but finite length genome, and an infinite length genome.

There are other situations where the eigenvectors of L_n are highly localized. For example, if the diagonal matrix R_n has distinct and, say, strictly monotonically increasing entries, then it is again the case that, for small enough $\|M_n\|$, the eigenvectors are highly localized. What distinguishes this case from the random case is that now the overlaps in the eigenvectors are highly correlated with the

difference in eigenvalue: if $|\lambda_\alpha - \lambda_\beta|$ is small, then is very likely that the peak of ψ_α is close to the peak of ψ_β. This becomes quite important when we consider the effects of the non-linear corrections.

To the best of our knowledge, this precise situation has not yet been analyzed, though considerable effort has been devoted to studying analogous questions on the lattices $\mathbb{Z}^d$, and Anderson Localization has been rigorously established in many representative cases, see Ref. 17. In the physics literature it has been shown that Anderson Localization occurs for a system based on the Bethe lattice, see Ref. 1. This is of interest for us, as the Bethe lattice embeds isometrically into the hyperbolic plane. Hence this indicates that the more efficient diffusion, which occurs in negatively curved spaces, does not destroy Anderson Localization. We emphasize that we have not proved the assertion that these models exhibit Anderson Localization and so, in the final section, we give some numerical examples showing that these models display many of the qualitative properties of Anderson Localized systems.

4. WEAK GENETIC DIVERSITY

Before considering the role of non-linearities, we consider what a linear model satisfying the localization ansatz would predict. Let us fix a large value of n so that L_n has many exponentially localized, well separated eigenstates for eigenvalues near to λ_N. We follow the continuum model and explicitly include a scalar, F, in our system:

$$\frac{d\mathbf{P}}{dt} = (L_n + F)\mathbf{P}. \tag{16}$$

In a linear model, the addition of F has no qualitative effect on the population distribution, it simply scales the solution at time t by e^{tF}. As we shall see, this is no longer the case once we include non-linear corrections.

If $\mathbf{P}_0$ is an initial population distribution, then evolving under Eq. (16), the population satisfies:

$$\mathbf{P}(t) = \sum_\alpha \langle \mathbf{P}_0, \psi_\alpha \rangle \psi_\alpha e^{(F+\lambda_\alpha)t}. \tag{17}$$

The numbers $\{F + \lambda_\alpha\}$ are therefore the *replication rates* for the quasi-species $\{\psi_\alpha\}$.[4] For long times, only the terms with $F + \lambda_\alpha > 0$ make a significant contribution to $\mathbf{P}(t)$. The λ_N-term is still the dominant term, but there are many terms with $\lambda_N - \lambda_\alpha$ quite small, which therefore make significant contributions for a long time. Because these eigenstates are well localized *and* well separated,

[4] In this context we refer, by analogy, to all of the eigenvectors of L_n as quasi-species though they may be neither localized, nor mostly positive.

there can be different dominant terms at different locations in genotype space. Thus, even without non-linear corrections, a model satisfying the localization ansatz would exhibit some kind of genetic diversity, which we call *weak genetic diversity*.

5. NON-LINEAR EFFECTS

In Ref. 15 Nelson and Shnerb modify the model in (14) by adding, among other things, a non-linear term:

$$u_t(x,t) = (\mu\Delta + q(x) + F)u(x,t) - bu^2(x,t), \tag{18}$$

where $b > 0$. The effect of this term is to limit $u(x,t)$ from above. The analogue of the model in (18) is an equation of the form:

$$\frac{d\mathbf{P}(t)}{dt} = (L+F)\mathbf{P}(t) - b\mathbf{P}(t).*\mathbf{P}(t), \tag{19}$$

with $L = R_n + M_n$. Here we use the MATLAB® notation for component-wise vector multiplication: if $\mathbf{v} = (v_1, \ldots, v_m)$ and $\mathbf{w} = (w_1, \ldots, w_m)$, then $\mathbf{v}.*\mathbf{w} = (v_1w_1, v_2w_2, \ldots, v_mw_m)$. For this discussion we take n to be a fixed, sufficiently large integer and M_n given by (5), though much of what we say should remain true with any reasonable choice of mutation matrix.[5] One can add other non-linearities and obtain models with similar qualitative behavior. These models along with their basic mathematical properties are described in the Appendix.

The remarkable observation made by Nelson and Shnerb is that, if $\mu\Delta + q(x)$ (in (18)) exhibits Anderson localization, then the large time asymptotics of the non-linear equation actually depend on all the eigenvalues, $\{\nu_\alpha\}$, of $\mu\Delta + q(x)$ with $\nu_\alpha + F > 0$. If L satisfies the localization ansatz, then the asymptotic analysis used in Ref. 15 applies, *mutatis mutandis* to (19). We present their analysis, in our context.

The spectrum, $\{\lambda_\alpha\}$, of L is quite dense near to λ_N, and the corresponding eigenvectors, $\{\psi_\alpha\}$, are highly localized. As before we express the initial data as

$$\mathbf{P}(0) = \sum_\alpha \langle \mathbf{P}(0), \psi_\alpha\rangle \psi_\alpha = \sum_\alpha c_\alpha(0)\psi_\alpha, \tag{20}$$

[5] The analogue of (19), for the Eigen model, in the formulation given in Eq. (12), is:

$$\frac{d\mathbf{W}}{dt} = (L+F)\mathbf{W} - bR_n^{-\frac{1}{2}}\mathbf{W}.*\mathbf{W}, \tag{21}$$

with $L = \sqrt{R_n}Q_n\sqrt{R_n} - D_n$. Numerically, this model behaves very similarly to that defined in (19).

where $c_\alpha(t) = \langle \mathbf{P}(t), \psi_\alpha \rangle$. Under (18), these coefficients evolve according to:

$$\frac{c_\alpha(t)}{dt} = (F + \lambda_\alpha)c_\alpha(t) - b \sum_{\beta,\gamma} w_{\alpha,\beta\gamma} c_\beta(t) c_\gamma(t), \tag{22}$$

where

$$w_{\alpha,\beta\gamma} = \sum_j \psi_\alpha(j)\psi_\beta(j)\psi_\gamma(j). \tag{23}$$

We assume that F is selected so that the eigenvectors, ψ_α, corresponding to eigenvalues with $F + \lambda_\alpha \geq 0$, satisfy the localization properties enumerated above. Following Nelson and Shnerb, we further assume that the states with $F + \lambda_\alpha < 0$ are not relevant for the large time asymptotics. The localization ansatz implies that, if $F + \lambda_\alpha > 0$, and $|\lambda_\alpha - \lambda_\beta|$ is small, then, with high probability, unless $\alpha = \beta = \gamma$, $w_{\alpha,\beta\gamma}$ is very small. Letting $w_\alpha = w_{\alpha,\alpha\alpha}$ we see that therefore

$$\frac{dc_\alpha(t)}{dt} \approx (F + \lambda_\alpha)c_\alpha(t) - b w_\alpha c_\alpha^2(t). \tag{24}$$

We can solve (24) to obtain:

$$c_\alpha(t) = \frac{c_\alpha(0)e^{(F+\lambda_\alpha)t}}{1 + c_\alpha(0)\frac{bw_\alpha}{F+\lambda_\alpha}\left(e^{(F+\lambda_\alpha)t} - 1\right)}. \tag{25}$$

Hence as $t \to \infty$, all coefficients such that $F + \lambda_\alpha > 0$ have a finite, non-zero asymptotic value given by

$$\lim_{t\to\infty} c_\alpha(t) = \frac{F + \lambda_\alpha}{b w_\alpha}. \tag{26}$$

As each eigenvector, ψ_α, represents a distinct quasi-species, coupling localization in genotype space with a simple non-linearity produces a model exhibiting long time genetic diversity. As t tends to infinity, the model predicts a collection of distinct quasi-species, occupying different parts of genotype space, whose size is determined by F. This explains why we call F the environmental fecundity. In a situation like that described in Ref. 6, F would be a unimodal function of the productivity, increasing to a maximum and then falling off.

What distinguishes a random fitness matrix from one with monotonely increasing diagonal entries is that, in the latter case, the eigenvectors with significant overlaps in their supports tend to have nearby replication rates. Hence, when the non-linear terms are included, paths exist in the "replication landscape" defined by the coefficients $\{w_{\alpha,\beta\gamma}\}$, which give the population the opportunity to cascade toward quasi-species with lower replication rates. This claim is born out by the numerical simulations of the non-linear equation in the next section. In the random case, no such paths exist and this further supports our claim that these models will display stable genetic diversity. It also suggests a connection between these models

and an interesting percolation problem on a replication landscape defined by the spectral theory of L.

6. NUMERICAL EXPERIMENTS

In this section we present several numerical experiments. If the genome length is n, then the matrix size is $2^n \times 2^n$, hence, at present, we are limited to $n \leq 11$. This should be compared to a viral genome with size about $n = 10^5$ or the human genome, with size of $n = 3 \times 10^9$, hence, these experiments should be understood as merely illustrative.

In a variety of papers, notably in Ref. 20, it is shown that, in order for quasi-species to exist in the large n limit, it is necessary that $n\mu$ be less than the maximal diagonal term in the fitness matrix. For our numerical simulations we divide by n so that μ is fixed and

$$M_{ij} = \begin{cases} -\mu & \text{if } i = j \\ \frac{\mu}{n} & \text{if } d_H(i, j) = 1 \\ 0 & \text{otherwise.} \end{cases} \tag{27}$$

We then compute the eigenvalues and eigenvectors of matrices of the form $L = R + M$, where R is a diagonal matrix with (pseudo)random, uniformly distributed entries, scaled to lie in $[0, 1]$. Physically this amounts to replacing the time parameter t by t/n. For purposes of comparison, we also consider diagonal matrices with distinct but smoothly growing entries, e.g. $R_{ii} = \tanh(2^{-n}i)$, the "monotone" model, and fitness matrices arising in single peak fitness landscapes, $R_{ii} = 1/(1 + d_H(S_i, S_0))$, the "1-peak" model. Here $S_0 = (1, 1, \ldots, 1)$.

6.1. The Spectrum

For a given matrix L, let $\{\lambda_\alpha\}$ denote the spectrum and $\{\psi_\alpha\}$, the corresponding normalized eigenvectors. The eigenvalues are indexed in increasing order. In our experiments we see that, with a random fitness matrix, the spectrum is distributed fairly uniformly over an interval, with decreasing density near the upper endpoint, see Fig. 1. This is in agreement with known results on the spectral density function for Anderson localized systems in the continuum case, see Refs. 2 and 22.

6.2. Localization

The matrices we consider are symmetric, so the eigenvectors are real and orthonormal:

$$\sum_{k=1}^{2^n} \psi_\alpha(k)\psi_\beta(k) = \delta_{\alpha\beta}. \tag{28}$$

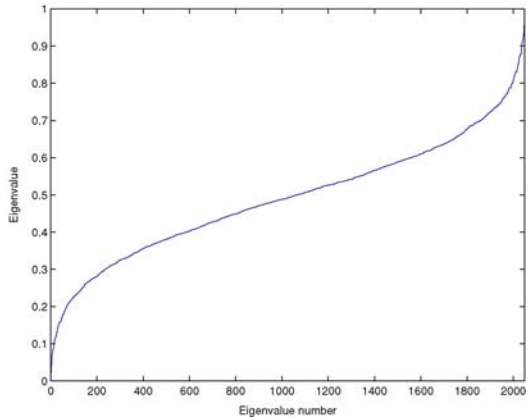

Fig. 1. The spectrum of a random model, with $n = 11$ and $\mu = 10^{-5}$.

To measure the extent of the localization of the eigenvectors we compute the cubic sum deficit

$$C_\alpha = 1 - \sum_{k=1}^{2^n} |\psi_\alpha(k)|^3. \tag{29}$$

If the eigenvectors were perfectly localized then C_α would be zero. If the eigenvectors were completely de-localized, then $C_\alpha = 1 - 2^{-\frac{n}{2}}$. To measure the localization of the eigenvectors, we compute the mean cubic sum deficit:

$$\overline{D3} = \frac{1}{2^n} \sum_{\alpha=1}^{2^n} \left[1 - \sum_{j=1}^{2^n} |\psi_\alpha(j)|^3 \right]. \tag{30}$$

Figure 2 shows the $\log_{10} \overline{D3}$, for three different types of fitness matrix as a function of $\log_{10} \mu$. The random and monotone models show localization and the 1-peak model does not. For $n = 10$ and $\mu = 0.0001$, we evaluated the cubic sum deficits $\{C_\alpha\}$ for a random and a monotone model. For the random model, and eigenvalues in the interval [0.8, 1], the numbers $C_\alpha < 4.5 \times 10^{-6}$. For the monotone model, $C_\alpha < 6.802 \times 10^{-4}$, for eigenvalues in this range. Hence near to the Perron-Frobenius eigenvalue, the random model is better localized than the monotone model.

6.3. Separation of Peaks

In the second set of experiments, we show that, for the random model, the supports of the eigenvectors with nearby energies are randomly distributed. As

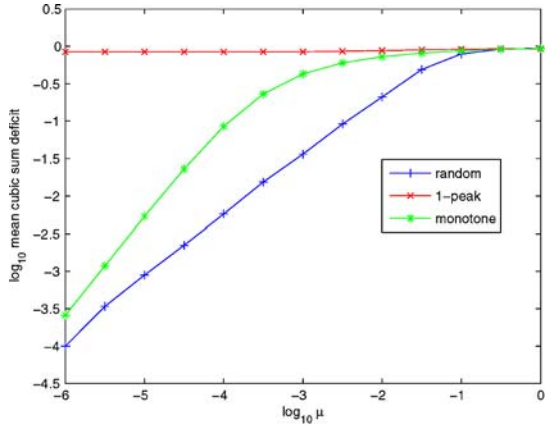

Fig. 2. The $\log_{10} \overline{D3}$, as a function of $\log_{10} \mu$, for 3 representative models with $n = 10$.

noted above, the indexing by $j \in \mathcal{J}_n$ is entirely arbitrary, so to demonstrate this we locate the peaks of the eigenvectors and plot the mean Hamming distance between peaks, for eigenvectors with eigenvalues that differ by at most 0.05.[6] If $j_\alpha \in \mathcal{J}_n$ is the index of the peak of ψ_α, then the plots in Fig. 3 show

$$\overline{d}_\alpha = \frac{\sum\limits_{\{\beta:\, |\lambda_\alpha - \lambda_\beta| < .05\}} d_H(S_{j_\alpha}, S_{j_\beta})}{\#\{\beta : \, |\lambda_\alpha - \lambda_\beta| < 0.05\}}, \tag{31}$$

with α along the horizontal axes, for both the random and the monotone models. Plots are shown for three different values of n with $\mu = 0.001$. We note that the random model behaves as if the peaks are uniformly distributed on $\mathcal{G}_n$, whereas, for the monotone model, the peaks of eigenvectors corresponding to nearby eigenvalues have a strong tendency to cluster.[7]

In Fig. 4 we show the actual Hamming distances between the peaks of the eigenvectors, for a random model and a monotone model with $n = 11$ and $\mu = 0.001$. The checkerboard plots in Fig. 4 show the distances for the eigenvectors corresponding to the 60 largest eigenvectors. The eigenvalue is decreasing from left to right and down to up in these figures. The distances in the random model are clearly much more randomly distributed than in the monotone case, and much more likely to be large.

[6] These operators are normalized so that their spectra lie in the interval [0, 1].

[7] For uniformly distributed points in $\mathcal{G}_n$, the expected distance between points is $n/2$ and the variance is $n/4$.

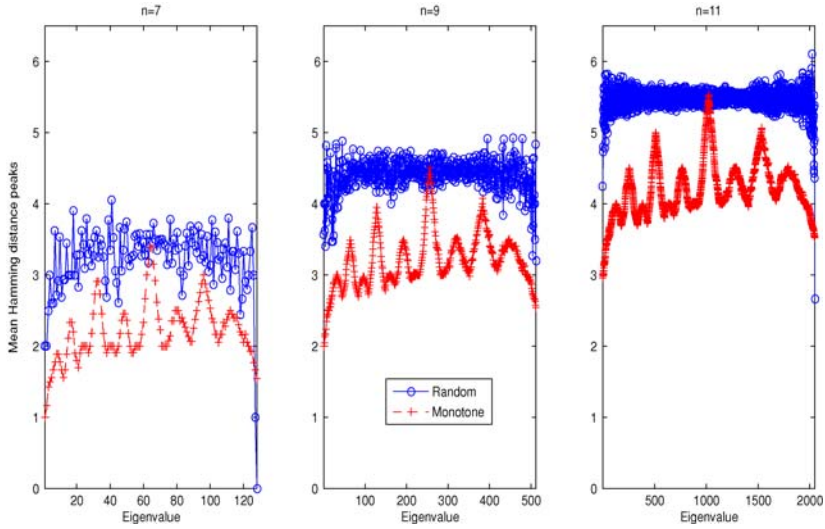

Fig. 3. The mean Hamming distance between the peaks of eigenvectors, with eigenvalue difference less than 0.05.

6.4. Non-Linear Models

In the third set of experiments we show runs of the non-linear model given in Eq. (19), with a random fitness matrix, a monotone fitness matrix, and a 1-peak fitness matrix. We use a genome of length $n = 8$, $b = .02$, and $\mu = .01$. The fecundity F is selected so that, for the random model, we expect an asymptotic population of 20. Each plot shows several time steps, with the asymptotic state (the outer envelope) shown in black. The horizontal axis is the genotype labeled by $\mathcal{J}_8$. In Fig. 5 we see that the random and 1-peak models each have essentially the predicted number of quasi-species, whereas the monotone model has a single, very broad, quasi-species. This would seem to be a result of cascading in the non-linear model, allowed by the proximity of the supports of eigenvectors with nearby eigenvalues.

The final set of figures shows the "phase transition" that occurs as the mutation rate is increased. Such phase transitions are typical of Anderson Localized systems. For Fig. 6(a), we solved Eq. (19) with $n = 8$, $b = .02$, and μ ranging from .001 to 100. For Fig. 6(b), we solved Eq. (21) for the Eigen model, with $n = 8, b = .02$, and $q = 8/(\mu + 8)$ for the same values of μ. The degradation matrix D has random entries lying in $[0, 0.2]$. We show the asymptotic population densities, $\mathbf{P}(\infty)/\sum_j P_j(\infty)$. The initial vector is $(1, \ldots, 1)$; as is clear from Eq. (26), any non-negative (non-trivial) initial datum produces the same asymptotic state. The

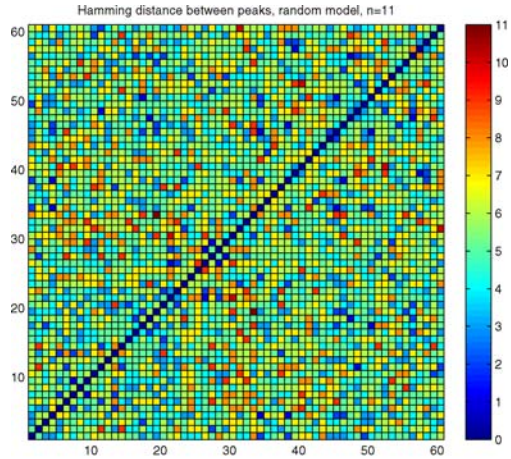

(a) A random model.

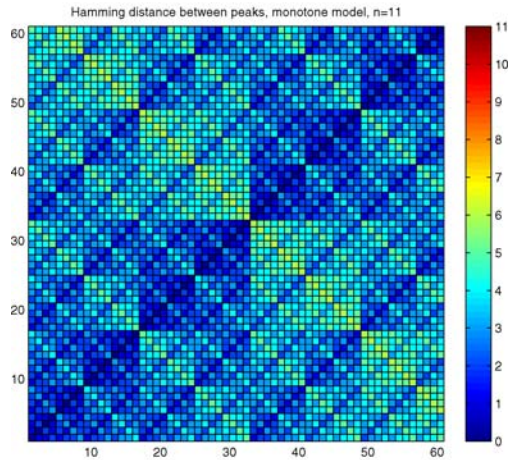

(b) A monotone model.

Fig. 4. The Hamming distances between the peaks of the eigenvectors corresponding to the 60 largest eigenvalues. The eigenvalues are listed in descending order with the lower left corner corresponding to (λ_N, λ_N).

transition from localized populations to de-localized populations is quite apparent. Of course, a true phase transition can only occur in the infinite n limit. The front axis shows that genotype labeled by $\mathcal{J}_8$. The scaled logarithm of the mutation rate is shown on the other horizontal axis.

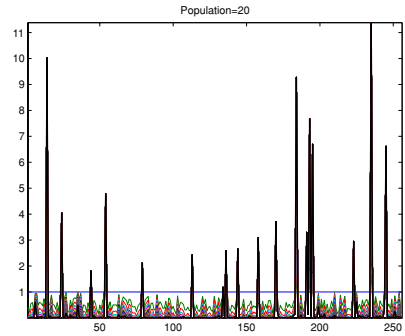

(a) A random model.

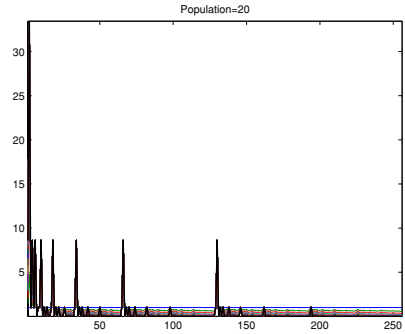

(b) A 1-peak model.

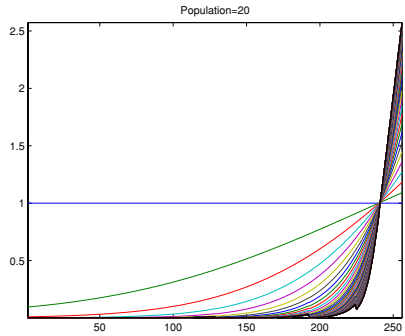

(c) A monotone model.

Fig. 5. Several time-steps of non-linear parallel models with different types of fitness matrices. The genotypes, interpreted as a binary numbers, appear on the horizontal axis, and the vertical axis shows the population density of each genotype.

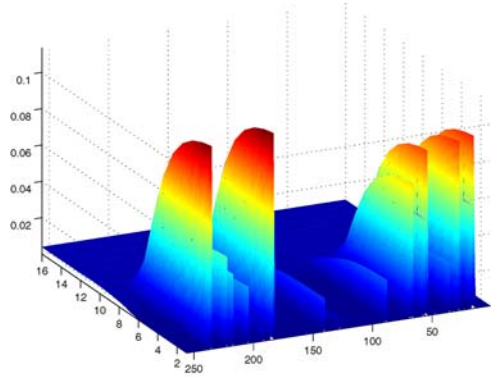

(a) The paramuse model

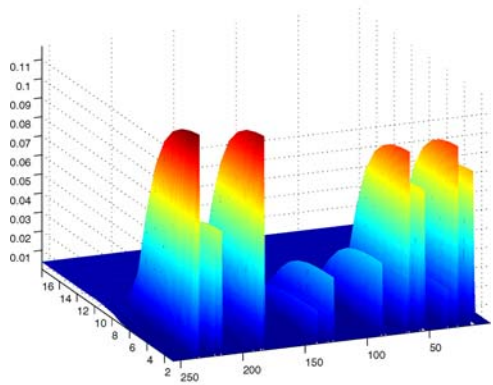

(b) The Eigen model

Fig. 6. Solutions of the non-linear models, 19 and 21, showing the population densities, with a variety of different mutation rates. The parameters are $n = 8$, $b = .02$, $\mathbf{P}_0 = (1, \ldots, 1)$. The fecundity F is selected so that $L + F$ has 20 positive eigenvalues. The "front" axis shows the genotypes, interpreted as binary numbers. The mutation rate, on a log-scale, is shown on the front-to-back horizontal axis. The vertical axis shows the asymptotic population densities $\mathbf{P}(\infty)/\langle \mathbf{P}(\infty), \mathbf{1} \rangle$.

APPENDIX A. MORE GENERAL CLASSES OF NON-LINEAR MODELS

Instead of the constant b in Eq. (18) we could use a positive $L + F$-super-harmonic function $B(x)$ to obtain the equation

$$u_t(x, t) = (L + F)u(x, t) - B(x)u^2(x, t). \tag{32}$$

The function $B(x)$ is $L + F$ super-harmonic if

$$(L + F)B(x) - B^3(x) < 0. \tag{33}$$

In this case the maximum principle shows that if initial data satisfies $u(x, 0) < B(x)$ for all x, then $u(x, t) < B(x)$ for all x and $t > 0$.

We can apply similar considerations to a somewhat larger class of models, in which we include a second non-linearity to limit the total population

$$u_t(x, t) = (L + F)u(x, t) - B(x)u^2(x, t) - pu(x, t) \int u(x, t)\, dx. \tag{34}$$

The second, non-local term, can be shown to impose a limit on the total population $\int u(x, t)dx$, which the first term does not do. One can also show that, so long as $B(x) > c > 0$, the asymptotic behavior of a non-negative solution of (34) is similar to that for Eq. (18). If $B \equiv 0$, then the model in (34) has many critical points, none stable and none with a large number of non-zero coefficients.

By analogy, we let $\mathbf{B}$ be a positive $L + F$-super-harmonic vector, that is

$$(L + F)\mathbf{B} - \mathbf{B}. * \mathbf{B}. * \mathbf{B} < 0.$$

If we replace Eq. (19) with

$$\frac{d\mathbf{P}(t)}{dt} = (L + F)\mathbf{P}(t) - \mathbf{B}. * \mathbf{P}(t). * \mathbf{P}(t), \tag{35}$$

and $0 \leq P_j(0) < B_j$ for all j, then $0 \leq P_j(t) < B_j$ for all j and $t > 0$. A model similar to 34 is given by

$$\frac{d\mathbf{P}(t)}{dt} = (L + F)\mathbf{P}(t) - \mathbf{B}. * \mathbf{P}(t). * \mathbf{P}(t) - \beta\langle \mathbf{P}, \mathbf{1}\rangle \mathbf{P}, \tag{36}$$

where $\beta > 0$ and $\mathbf{1} = (1, \ldots, 1)$. These models are all positivity preserving. Their basic mathematical properties are established in the next section. It seems a very interesting and important problem to find the biologically relevant non-linear correction terms, and understand how they interact with an Anderson localized linear model.

APPENDIX B. MATHEMATICAL RESULTS

We consider models of the following general type:

$$\frac{d\mathbf{P}}{dt} = L\mathbf{P} - \mathbf{B}. * \mathbf{P}. * \mathbf{P} - \beta\langle \mathbf{P}, \mathbf{1}\rangle \mathbf{P} \tag{37}$$

where $\mathbf{B}$ is a pointwise positive, super-harmonic vector and β is a non-negative number. Here $L = \Lambda + A$, where Λ is a diagonal matrix and A is a matrix with zeroes on the diagonal and non-negative entries off the diagonal. This splitting of L into diagonal and non-diagonal parts is a little different from that used in the main article, but should not lead to confusion.

In order for such an equation to define a reasonable population model, it is necessary that it be positivity preserving. That is, if the initial data $\mathbf{P}(0)$ has

non-negative entries, then $\mathbf{P}(t)$ is non-negative for all $t > 0$. The models of the type given in (37) have this property. This is established in two steps and uses the Kato-Trotter product formula and its non-linear generalization.

We first treat the linear part. The solution to the linear equation $\partial_t \mathbf{P} = L\mathbf{P}$ is given by

$$\mathbf{P}(t) = e^{tL}\mathbf{P}(0) = e^{t(\Lambda+A)}\mathbf{P}(0), \tag{38}$$

where the matrix exponential is given by the usual formula, e.g.

$$e^{tB} = \sum_{j=0}^{\infty} \frac{(tB)^j}{j!}. \tag{39}$$

From this expression it is immediate that e^{tA} has non-negative entries for every $t > 0$. Indeed for the models considered above e^{tA} has positive entries for all $t > 0$. Because Λ and A do not commute, it does not follow immediately that $e^{tL} = e^{t(\Lambda+A)}$ also has positive entries. To prove this we use the Kato-Trotter product formula, which states that

$$e^{t(\Lambda+A)} = \lim_{n\to\infty} \left[e^{\frac{t}{n}\Lambda} e^{\frac{t}{n}A}\right]^n. \tag{40}$$

As the right hand side expresses e^{tL} as a limit of products of matrices with positive entries, it follows that e^{tL} also has non-negative entries. With a little more care we can show that, in fact, e^{tL} has positive entries. Hence the linear model is positivity preserving. For a thorough discussion of positivity preserving operators see section XII.12 of Ref. 19.

In Ref. 21 a non-linear generalization of the Kato-Trotter formula is given for non-linearities including the type in (37). We first observe that the vector field defined on $\mathbb{R}^{2^n}$ by

$$X(\mathbf{P}) = -\mathbf{B}.*\mathbf{P}.*\mathbf{P} - \beta\langle\mathbf{P}, \mathbf{1}\rangle\mathbf{P} \tag{41}$$

is tangent to the coordinate hyperplanes $\{\mathbf{P} : P_j = 0\}$, and therefore the positive orthant, $\{\mathbf{P} : P_j > 0 \text{ for all } j\}$, is invariant under the flow generated by this vector field. From this and the fact that the right hand side in (41) is negative in the positive orthant, it follows that if we start with non-negative initial data, then the equation

$$\frac{d\mathbf{P}}{dt} = X(\mathbf{P}), \tag{42}$$

has a unique bounded solution for all $t > 0$. Let $\mathcal{X}^t\mathbf{P}(0)$ denote the solution to (42) with initial data $\mathbf{P}(0)$. In Ref. 21 it is shown that the solution to (37) can be obtained as the following limit:

$$\mathbf{P}(t) = \lim_{n\to\infty} \left[e^{\frac{t}{n}L}\mathcal{X}^{\frac{t}{n}}\right]^n \mathbf{P}(0). \tag{43}$$

As $\mathcal{X}^t$ is positivity preserving and e^{tL} is positivity improving, it follows that the equation in (37) is also positivity preserving. A small modification of this formula, useful for numerical simulations is called "Strang's splitting:"

$$\mathbf{P}(t) = \lim_{n\to\infty} \left[\mathcal{X}^{\frac{t}{2n}} e^{\frac{t}{n}L} \mathcal{X}^{\frac{t}{2n}}\right]^n \mathbf{P}(0). \tag{44}$$

We now consider the constraints imposed on the solution by the non-linearities. Assuming that $\mathbf{P}(t)$ is non-negative, it follows that there is a constant C such that

$$\langle L\mathbf{P}, \mathbf{1}\rangle \leq C\langle \mathbf{P}, \mathbf{1}\rangle. \tag{45}$$

Thus, a non-negative solution to (37) satisfies the differential inequality:

$$\frac{d\langle \mathbf{P}, \mathbf{1}\rangle}{dt} \leq C\langle \mathbf{P}, \mathbf{1}\rangle - \beta\langle \mathbf{P}, \mathbf{1}\rangle^2. \tag{46}$$

This easily implies that if the initial population $\langle \mathbf{P}(0), \mathbf{1}\rangle < \beta^{-1}C$, then the total population never exceeds $\beta^{-1}C$. Moreover, if the population initially exceeds this value, then it decreases at time goes by. Combining this observation with the positivity preserving property, we deduce that, with non-negative initial data, the solution to (37) exists for all $t > 0$.

For the other non-linearity we use the hypothesis that A has non-negative entries off the main diagonal. We suppose that $P_j(0) < B_j(0)$ for all j. Suppose that there were a j_0 and a first $t_0 > 0$, where $P_{j_0}(t_0) = B_{j_0}(t_0)$. In this case it would still be true that $P_j(t_0) \leq B_j(t_0)$, for all j. Hence, our assumption on A and the fact that the remaining terms in L are diagonal, would imply that

$$(L\mathbf{P}(t_0))_{j_0} \leq (L\mathbf{B})_{j_0}. \tag{47}$$

As the solution is non-negative this would imply the differential inequality

$$\left(\frac{dP_{j_0}(t_0)}{dt}\right) \leq (L\mathbf{B})_{j_0} - (\mathbf{B}.*\mathbf{B}.*\mathbf{B})_{j_0} < 0 \tag{48}$$

The last inequality is because $\mathbf{B}$ is assumed to be super-harmonic. But this contradicts the assumption that $P_{j_0}(t) < P_{j_0}(t_0)$, for $t < t_0$.

To sum up we have proved the following theorem:

Theorem 1. *If* $\mathbf{P}(0)$ *is non-negative, then the solution,* $\mathbf{P}(t)$, *to (37) exists for all time and remains non-negative. If* $\langle \mathbf{P}(0), \mathbf{1}\rangle < \beta^{-1}C$, *then this remains true for all time, and in any case remains bounded. If* $\mathbf{B}$ *is a positive super-harmonic vector,* $L\mathbf{B} - \mathbf{B}.*\mathbf{B}.*\mathbf{B} < 0$, *and* $P_j(0) < B_j$, *for all* j, *then this inequality remains true for all* $t > 0$.

It is likely that by treating the two non-linearities together, rather than separately as done above, more precise constraints could be obtained.

ACKNOWLEDGMENTS

The author would like to thank Ben Mann for insisting that I participate in the FUNBIO program and securing the funding to make it happen. I am very thankful to all participants in the DARPA FUNBIO workshops and most especially to Richard Lenski, Sally Otto, Michael Deem, Jeong-Man Park, Chris Adami, and Jack Morava for sharing their ideas on biology and evolution with me. I would also like to thank Michael Deem, Richard Lenski, and Claus Wilke for their suggestions for improvement of earlier drafts. I am grateful to Harvey Rubin for telling me the biochemical facts of life and to John Schotland for his considerable help with statistical mechanics and many useful suggestions related to this work. Finally, I thank the referees for their useful suggestions.

REFERENCES

1. R. Abou-Chacra, P. W. Anderson and D. J. Thouless, A self consistent theory of localization. *J. Phys.C: Solid St. Phys.* **6**:1734–1752, (1973).
2. P. W. Anderson, Absence of diffusion in certain random lattices. *Phys. Rev.* **109**:1492–1505, (1958).
3. P. W. Anderson, Suggested model for prebiotic evolution: The use of chaos. *Proc. Natl. Acad. Sci.* **80**:3386–3390, (1983).
4. E. Baake, M. Baake and H. Wagner, Ising quantum chain is equivalent to a model of biological evolution. *Phys. Rev. Lett.* **78**:559–562, (1997).
5. R. Carmona and J. Lascoux, *Spectral Theory of Random Schrödinger Operators*, (Birkhäuser, Boston-Basel-Berlin, 1990).
6. S. S. Chow, C. O. Wilke, C. Ofria, R. E. Lenski and C. Adami, Adaptive radiation from resource competition in digital organisms. *Science* **305**:84–86, (2004).
7. J. F. Crow and M. Kimura, *An Introduction to Population Genetics Theory*, (Harper and Row, New York, 1970).
8. M. Eigen, Molekulare Selbstorganisation und Evolution (Self organization of matter and the evolution of biological macro molecules.). *Naturwissenshaften* **58**:465–523, (1971).
9. M. Eigen, J. McCaskill and P. Schuster, Molecular quasi-species. *J. Phys. Chem.* **92**:6881–6891, (1988).
10. M. Eigen, J. McCaskill and P. Schuster, The molecular quasi-species. *Adv. Chem. Phys.* **75**:149–263, (1989).
11. M. Eigen and P. Schuster, A principle of natural self-organization. Part A. emergence of the hyper cycle. *Naturwissenschaften* **64**:541–565, (1977).
12. J. Hermisson, H. Wagner and M. Baake, Four-state quantum chain as a model for sequence evolution. *J. Stat. Phys.* **102**:315–343, (2001).
13. K. Jain and J. Krug, Adaptation in simple and complex fitness landscapes. arXiv:q-bio, PE/0508008 **v1**:1–42, (2005).
14. J. McCaskill, A localization threshold for macromolecular quasi-species from continuously distributed replication rates. *J. Chem. Phys.* **80**:5194–5202, (1984).
15. D. R. Nelson and N. M. Shnerb, Non-Hermitian localization and population biology. *Phys. Rev. E* **58**:1383, (1998).
16. J.-M. Park and M. W. Deem, Schwinger Boson formulation and solution of the Crow-Kimura and Eigen models of quasispecies theory, submitted. *J. Stat. Phys.* 1–33, (2006).

17. L. A. Pastur and A. Figot, *Spectra of Random and Almost Periodic Operators*, (Springer Verlag, Berlin-Heidelberg-New York, 1992).
18. P. B. Rainey and M. Travisano, Adaptive radiation in a heterogeneous environment. *Nature* **394**:69–72, (1998).
19. M. Reed and B. Simon, *Methods of Modern Mathematical Physics VI: Analysis of Operators*, (Academic Press, New York-San Francisco-London, 1978).
20. D. B. Saakian, E. Muñoz, C.-K. Hu, and M. W. Deem, Quasispecies theory for multiple-peak fitness landscapes. *Phys. Rev. E* **73**:041913-1–10, (2006).
21. M. E. Taylor, *Partial Differential Equations, Vol. 3, vol. 117 of Applied Mathematical Sciences*, (Springer, New York, 1996).
22. D. J. Thouless, Anderson's theory of localized states. *J. Phys.C: Solid St. Phys.* **3**:1559–1566, (1970).
23. H. Wagner, E. Baake and T. Gerisch Ising quantum chain and sequence evolution. *J. Stat. Phys.* **92**:1017–1052, (1998).